Journal of Mining and Environment (JME) Vol. 17, No. 5, 2026, 1715-1735

Shahrood University of Technology

Journal of Mining and Environment (JME)

Journal homepage: www.jme.shahroodut.ac.ir

Iranian Society of Mining Engineering (IRSME)

Mine-To-Mill Integration of Blasting Parameters and Size-Based Production Using Optimized ANNs: A Case Study of Sar-Asiab Limestone Complex, Iran

Mojtaba Saeidi[1], Vahideh Shojaei[1*], Hamid Khoshdast[1], and Alireza Gholami[2]

1. Department of Mining Engineering, Higher Education Complex of Zarand, Shahid Bahonar University of Kerman, Kerman, Iran
2. The Robert M. Buchan Department of Mining, Queen's University, Kingston, Ontario, Canada

Article Info

Received 2 February 2026

Received in Revised form 16 June 2026

Accepted 4 August 2026

Published online 4 August 2026

DOI: 10.22044/jme.2026.17439.3463

Keywords

Blasting optimization

Mine-to-mill integration

Artificial neural networks

Fragmentation prediction

Sensitivity analysis

Abstract

Effective blast design is crucial for downstream comminution efficiency. However, modeling its impact on size-based production remains challenging due to complex, non-linear rock–fragmentation interactions. This study developed an integrated mine-to-mill framework using optimized Artificial Neural Networks (ANNs) to predict total and size-fractioned production (0–40 mm, 40–80 mm) from blasting parameters at the Sar-Asiab Limestone Complex, Iran. The dataset comprises 55 real industrial observations after preprocessing. Two optimization algorithms, Genetic Algorithm (GA) and Particle Swarm Optimization (PSO), were employed to enhance ANN performance. The PSO-optimized ANN demonstrated significantly superior generalization, achieving a testing RMSE of 1341.8 (vs. 1549.5 for GA), an MAE of 1108.9 (vs. 1260.4), and an R^2 of 0.9487 (vs. 0.8937). Sensitivity-based feature importance analysis quantified the dominant predictors: explosive quantity (Emulite) contributed 18.4%, the number of boosters 14.9%, and key geometric parameters (mean hole depth, diameter, and spacing) collectively accounted for over 41%. In contrast, initiation system variables such as cortex length showed high linear correlation (r = –0.91) but minimal predictive importance (1.5%). These results underscore that explosive energy and its distribution, not just initiation configuration, are the primary drivers of size-based output. This data-driven framework provides a practical tool for aligning blast design with processing needs, directly supporting energy reduction and production stability in open-pit mining.

1. Introduction

Blasting is one of the most influential and energy-intensive operations in surface mining and plays a decisive role in determining the efficiency of downstream loading, hauling, crushing, and screening processes [1–3]. The fragmentation characteristics generated during blasting directly affect crusher throughput, comminution energy consumption, equipment utilization, and overall mine productivity [4–8]. Consequently, blasting is no longer regarded as an isolated rock breakage process but as the first stage of an integrated mine-to-mill system, where upstream blasting decisions significantly influence downstream processing performance [9–11]. Achieving optimal blasting performance remains a challenging task because blasting outcomes are controlled by complex interactions among blast geometry, explosive characteristics, initiation systems, and site-specific geological conditions [12,13]. These interactions are highly non-linear and often difficult to represent using traditional empirical or statistical approaches. Although conventional regression-based methods have been successfully used for preliminary blast design and fragmentation assessment, their predictive capability is often limited when applied to dynamic industrial environments characterized by multiple interacting variables [14].

To overcome these limitations, artificial intelligence (AI) techniques have been increasingly

Corresponding author: v.shojaei@uk.ac.ir (V. Shojaei)

adopted in mining and blasting engineering [15–18]. Among these techniques, Artificial Neural Networks (ANNs) have attracted considerable attention because of their ability to learn complex non-linear relationships directly from operational data without requiring explicit physical assumptions [16–18]. ANN-based models have been successfully applied to predict blast fragmentation, estimate blasting costs, assess environmental impacts, and forecast production-related variables. However, ANN performance is highly dependent on network architecture and hyperparameter selection, which has motivated the use of advanced optimization techniques for ANN training and configuration [19].

Evolutionary and swarm-based optimization algorithms, particularly Genetic Algorithms (GA) and Particle Swarm Optimization (PSO), have therefore become popular tools for improving ANN performance [20–22]. These algorithms enhance ANN learning by optimizing network parameters and reducing the risk of convergence to local minima. As a result, hybrid ANN-GA and ANN-PSO models have been widely applied to blasting-related prediction problems.

Recent studies demonstrate the growing importance of hybrid AI approaches in blasting engineering. Saubi et al. [23] compared ANN, ANFIS, ANN-GA, and ANN-PSO models for fragmentation prediction and reported superior performance of the PSO-optimized ANN. Gebretsadik et al. [25] employed machine learning methods to predict rock fragmentation and identified powder factor as the dominant predictor. Bai et al. [26] developed a multi-objective PSO framework for blasting parameter optimization and vibration reduction. Guo et al. [28] and Bisoyi and Pal [29] proposed intelligent optimization frameworks for fragmentation prediction in open-pit mines, while Huan et al. [31] introduced interpretable deep learning approaches for estimating mean fragmentation size. Collectively, these studies confirm the effectiveness of AI-based methods for modeling blasting outcomes.

Despite these advances, a careful review of the literature reveals several important gaps. First, the majority of ANN-GA/PSO blasting studies focus primarily on conventional fragmentation indicators such as mean fragment size, fragmentation index, blastability parameters, or environmental impacts [23,25,26,28–31]. Although these outputs are important, they do not directly represent the production variables that govern the performance of crushing and screening circuits. As a result, the practical connection between blast design and downstream production performance remains insufficiently addressed. Second, many published ANN-based blasting studies emphasize predictive accuracy while providing limited interpretation of the underlying physical mechanisms governing model predictions [34–37]. Consequently, the resulting models often function as black-box predictors whose practical value for operational decision-making remains restricted. Third, although both GA and PSO have been extensively used to optimize ANN models, direct comparisons between ANN-GA and ANN-PSO under identical industrial datasets, identical input variables, identical validation procedures, and identical evaluation criteria remain relatively scarce. In many studies, conclusions regarding the superiority of one optimization strategy over another are difficult to generalize because different datasets, objectives, and performance metrics are employed.

Finally, most existing studies treat blasting as an isolated process and do not explicitly integrate blasting design variables with downstream production-oriented mine-to-mill objectives [9–11,27,32,33]. This limits the ability of such models to support holistic optimization of mining operations. To highlight the distinction between the present work and previous ANN-GA/PSO blasting studies, Table 1 summarizes the main characteristics of representative studies reported in the literature.

Table 1. Comparison between representative ANN-GA/PSO blasting studies and the present research

Study	Main Prediction Target	Mine-to-Mill Perspective	Direct GA–PSO Comparison	Feature Importance Analysis	Size-Class Production Prediction
Saubi et al. [23]	Fragmentation indicators	No	Yes	Yes	No
Gebretsadik et al. [25]	Fragmentation extent	No	No	Yes	No
Bai et al. [26]	Fragmentation and vibration	No	No	Limited	No
Guo et al. [28]	Fragmentation prediction	No	No	Limited	No
Bisoyi and Pal [29]	Fragmentation optimization	No	No	No	No
Huan et al. [31]	Mean fragmentation size	No	No	Yes	No
Present study	Size-based production (0–40 mm and 40–80 mm)	Yes	Yes (same industrial dataset)	Yes	Yes

The novelty of the present study therefore does not lie in merely applying ANN, GA, or PSO algorithms, since such approaches have already been reported in the blasting literature. Instead, the novelty arises from the integration of these methods within a production-oriented mine-to-mill framework. Specifically, this study contributes to the literature through four interconnected innovations:

1. Direct prediction of operationally relevant size-based production outputs (0–40 mm and 40–80 mm tonnages) rather than conventional fragmentation indices.
2. Development of an integrated mine-to-mill modeling framework that explicitly links blasting design parameters with downstream crushing and screening performance.
3. A rigorous head-to-head comparison of GA-optimized and PSO-optimized ANN models using the same industrial dataset, identical input variables, identical validation procedures, and identical evaluation metrics.
4. Integration of sensitivity-based feature importance analysis to quantify the relative contribution of blasting variables and provide physically interpretable insights into blasting–production relationships.

Based on these motivations, the objective of this study is to develop and evaluate optimized ANN models for predicting total production and size-class production outputs at the Sar-Asiab Limestone Complex, Iran. Two ANN optimization strategies, namely GA and PSO, are investigated and compared using identical datasets and evaluation protocols. In addition, feature importance analysis is employed to identify the dominant blasting variables controlling production performance. The resulting framework provides both predictive capability and engineering interpretability, thereby supporting more effective mine-to-mill optimization and data-driven blasting design.

2. Materials and Method

2.1. Short description of the studied mining site

The Sar-Asiab Limestone Complex lies 45 km southwest of Zarand in Kerman Province, Iran. Its limestone deposit holds an estimated 90 million tons of economically extractable reserves, making it one of the largest limestone mines in Iran. The operation employs conventional open-pit mining equipment with a daily production rate of 4000 t. In mining operations, drilling and blasting represent the foundational stage following mine planning. Their influence extends across downstream processes, including crushing, underscoring their critical role in final efficiency. Economic optimization of mining activities necessitates prioritizing blasting optimization. A key factor in this process involves analyzing how blasting variables—such as charge design and fragmentation patterns—affect the size distribution of broken ore, which directly impacts crushing performance and operational costs. After blasting and loading, as-mined ore with a maximum size of 75 cm is directed to a jaw crusher with a nominal capacity of 500 t/h for primary crushing. The operating discharge opening of the crusher is set at 80 cm to supply a product with d_{80} of 70 cm. To better manage feed supply to the processing unit and minimize downtime, the crusher's operating schedule is coordinated with the mine plan. The crushed ore is then directed to a double-deck vibrating screen to produce two sized products: 0–40 mm and 40–80 mm.

2.2. Data collection and dataset preparation

The data for this research were collected from the mining and comminution sectors at the Sar-Asiab Limestone Complex. Through a combination of plant inspections and extensive research, several critical parameters were identified as primary factors influencing the total and incremental (0–40 mm and 40–80 mm) production rates. These include key blasting parameters: level of exploited blocks, spacing length and height, diameter, depth and number of holes, number of boosters, type and quantity of explosives, number of caps, and blasting type (normal, electric, and Nonel). These variables were derived from operational data captured by the comminution control system (specifically screening products) alongside daily operational records from mining operations related to blasting parameters. Drawing from these findings, the current study establishes a predictive model built on a consolidated dataset that combines critical blasting variables with core operational metrics. After preprocessing (removing rows with missing values and columns containing zero values), the final cleaned dataset consists of 55 complete observations, each containing 12 input blasting parameters and 3 output production variables (total tonnage, 0–40 mm, and 40–80 mm).

2.3. Pre-processing Dataset

During the modeling phase, data normalization is critical to minimize the influence of scale

discrepancies caused by differing magnitudes and measurement units among feature variables. Subsequently, all variables were merged into a unified dataset. To preserve data integrity, rows with missing values and columns containing zero values were systematically excluded, yielding a final dataset of 55 observations. For standardization, the rescaling method was applied, and the derived equation is presented below [36]:

$$S_i = \frac{X_i - \min(X)}{\max(X) - \min(X)} \quad (1)$$

where S_i is the normalized dataset of X_i, X_i is the dataset in the dataset, max(X) and min(X) are the maximum and minimum values in X_i, respectively.

2.4. Correlation matrix development

To analyze interrelationships among variables in the dataset, a correlation matrix was used to quantify the strength and direction of associations using the Pearson correlation coefficient. This coefficient, denoted as r, ranges between –1 and 1, where values closer to 1 indicate a strong positive linear relationship (both variables tend to increase together). Conversely, values approaching –1 reflect a strong negative relationship (one variable decreases as the other increases). A coefficient of 0 suggests no discernible linear association [39]. The Pearson coefficient is mathematically defined as the covariance of two variables divided by the product of their standard deviations. This metric is particularly valuable for identifying redundant variables or multicollinearity in predictive modeling. In practical terms, high correlations ($|r| > 0.7$) may warrant feature selection to avoid overfitting, while weaker correlations ($|r| < 0.3$) highlight variables with minimal predictive influence. Such insights guide data preprocessing decisions, ensuring robustness in subsequent statistical analyses or machine learning workflows. By contextualizing these relationships, the matrix serves as a foundational tool for hypothesis validation and dimensionality reduction in complex datasets. The Pearson coefficient can be estimated using the following equation [40]:

$$r = \sum_{i=1}^{N} (X_i - \bar{X})(Y_i - \bar{Y}) / \sqrt{\sum_{i=1}^{N} (X_i - \bar{X})^2} \sqrt{\sum_{i=1}^{N} (Y_i - \bar{Y})^2} \quad (2)$$

where X_i and Y_i are the data of two groups of characteristic variables in the dataset, and N is the sample number of characteristic variables X_i and Y_i. While the correlation matrix reveals linear dependencies among blasting parameters, a more robust understanding of their predictive power requires non-linear modeling. The following section describes the ANN-based optimization framework employed in this study.

2.5. ANN modelling route

2.5.1. Optimization strategies

ANNs are powerful computational models capable of capturing complex patterns and relationships within data. However, the performance of an ANN largely depends on its architecture and the careful tuning of various parameters, such as the number of hidden layers, the number of neurons within each layer, learning rates, and activation functions. This fine-tuning process is crucial because suboptimal parameters can lead to overfitting, underfitting, or longer convergence times, thereby affecting the model's accuracy and efficiency. Given the complexity and non-linear nature of ANNs, parameter tuning is often a challenging task that requires exploring vast search spaces. Manual tuning is time-consuming and may not guarantee optimal results. Therefore, optimization algorithms such as GA and PSO are employed to automate the tuning process. These algorithms enhance the modeling capability of ANNs by systematically exploring the parameter space to identify the optimal set that minimizes errors and maximizes performance. Using optimization techniques not only accelerates model building but also improves robustness and generalization. By automating parameter selection, these methods adaptively find the best architecture and hyperparameters, reducing human bias and effort. This is where GA and PSO come into play as valuable tools for tuning ANNs, enabling more efficient and accurate modeling of complex datasets. In this research, PSO and GA were employed to develop ANN models aimed at estimating the output tonnage of two critical size fractions: 40–80 mm and 0–40 mm. By optimizing the neural network parameters using these techniques, the models can provide more accurate predictions of these size distributions, which are crucial for evaluating blasting process performance. The following sections introduce

each optimization algorithm in detail, highlighting their implementation and role in enhancing the ANN models.

2.5.2. Genetic optimization in ANN

Genetic optimization, an evolutionary algorithm inspired by natural selection, is a powerful tool for optimizing complex problems, including the training and configuration of ANNs. In this approach, a population of candidate solutions is iteratively evolved to achieve better performance, guided by a fitness function that evaluates how well each solution solves the target problem. The algorithm proceeds through cycles of selection, crossover (recombining parts of two solutions), and mutation (introducing random variations) to explore the solution space. In the context of ANNs, GAs are employed to optimize various aspects of the network, such as weights, biases, and even the architecture itself, including the number of layers and neurons [41]. This optimization enhances the network's ability to model complex, non-linear relationships in data, leading to improved accuracy and generalization. One of the primary advantages of using GA in ANN training is its ability to avoid local minima, a common challenge in traditional gradient-based optimization methods. By exploring a broader range of potential solutions through genetic variation, GAs are less likely to become trapped in suboptimal configurations, thus leading to more effective learning [42]. Additionally, GA is particularly beneficial when the search space is large and poorly understood, as it does not require gradient information and can handle discontinuous, non-differentiable, or noisy objective functions. This makes GA a versatile and robust method for optimizing ANNs, especially in scenarios where other optimization techniques might struggle. Moreover, GA is inherently parallelizable, allowing for efficient exploration of multiple solutions simultaneously, which can significantly reduce computational time in large-scale problems.

2.5.3. Particle swarm optimization (PSO) in ANN

PSO is a population-based stochastic optimization technique inspired by the social behavior of birds flocking or fish schooling. In PSO, a group of particles (potential solutions) moves through the solution space, with each particle adjusting its position based on its own experience and that of its neighbors. This movement is guided by two main factors: the particle's own best-known position and the global best-known position found by the swarm. These factors help each particle explore and exploit the solution space efficiently. When applied to ANNs, PSO is used to optimize network parameters such as weights and biases by minimizing an error function that quantifies the difference between predicted and actual outputs. PSO's ability to balance exploration and exploitation makes it particularly effective for finding high-quality solutions in complex, multi-dimensional spaces [24]. One of the key advantages of using PSO for optimizing ANNs is its simplicity and ease of implementation, as it requires fewer parameters to adjust compared to other techniques like GA or gradient-based methods. PSO is also highly adaptable to various types of objective functions, including non-differentiable, noisy, or discontinuous functions, making it a robust choice for ANN training in diverse applications. Furthermore, PSO's collaborative nature allows it to avoid local minima more effectively than traditional gradient-based methods, leading to more reliable and accurate models [43]. The inherent parallelism in PSO also contributes to its efficiency, as multiple particles can explore different regions of the solution space simultaneously, which is particularly beneficial for large-scale ANNs or complex optimization landscapes. Thus, PSO provides a powerful and flexible approach to optimizing ANNs, enhancing their performance across a wide range of tasks.

2.5.4. Modelling procedure

After implementing two separate ANN models in MATLAB 2021, the data were split into three sets: 70% for training, 10% for validation, and 20% for testing. This split was performed randomly but kept consistent across both GA and PSO optimizations to ensure fair comparison. Both models used 12 input parameters to predict two outputs, specifically the tonnage of 40–80 mm and 0–40 mm fractions. The goal was to use different optimization algorithms, GA for one model and PSO for the other, to identify which approach results in a more accurate and robust prediction model.

For the GA-optimized ANN:

- Network architecture: 2 hidden layers, each with 20 neurons (fully connected).
- Activation function: hyperbolic tangent (tanh) for all hidden layers; linear activation for output layer.

- Learning rate: 0.01.
- Optimization objective: minimize MSE on training data.
- Stopping criteria: maximum of 500 epochs (determined by GA as optimal); additionally, training stopped early if validation loss did not decrease for 50 consecutive epochs (early stopping).
- Number of independent runs: 30 to account for stochasticity; the model with the lowest validation error was selected.
- Overfitting prevention: early stopping based on validation set (10% of data) + L2 weight regularization ($\lambda = 0.001$).

For the PSO-optimized ANN:

- Network architecture: 3 hidden layers, each with 15 neurons (fully connected).
- Activation function: ReLU (Rectified Linear Unit) for hidden layers; linear for output.
- Learning rate: 0.005.
- Stopping criteria: maximum of 600 epochs (PSO-optimized) with early stopping patience of 60 epochs on validation loss.
- Number of independent runs: 30; best model selected based on validation MSE.
- Overfitting prevention: early stopping + dropout (rate = 0.2) after each hidden layer to reduce co-adaptation of neurons.

Both optimization algorithms (GA and PSO) were configured with a population size of 50 and run for 100 generations to tune the ANN hyperparameters (number of layers, neurons, learning rate, activation function, and regularization strength). The search space was defined as: hidden layers 1–4, neurons per layer 5–50, learning rate 0.001–0.1, and dropout 0–0.5. For GA, crossover probability = 0.8, mutation rate = 0.05. For PSO, inertia weight = 0.7, cognitive and social coefficients = 1.5 each. The differing architectures and parameters highlight the unique advantages each optimization algorithm offers when applied to neural network training. To ensure statistical robustness, the following additional measures were implemented:

- Instead of a single train/validation/test split, a stratified 5-fold cross-validation (CV) scheme was applied to the training+validation portion (80% of data) for hyperparameter selection. The final hold-out test set (20%) was never used during CV. For each fold, the model was trained on 4 folds and validated on the remaining 1 fold; performance was averaged across folds. This procedure was repeated 10 times with different random seeds to account for sampling variability.
- After hyperparameter selection via CV, each optimized model (GA-ANN and PSO-ANN) was retrained 30 times with different random weight initializations on the full training+validation set. For each run, the model was evaluated on the same unseen test set. The mean ± standard deviation of each performance metric (RMSE, MAE, R^2) across the 30 runs is reported in Section 3.3.
- Statistical significance of the difference between GA-ANN and PSO-ANN was tested using a paired t-test (since both models were evaluated on identical test set predictions across 30 independent runs). A p-value < 0.05 was considered statistically significant.
- Uncertainty quantification: The prediction intervals for individual test samples were estimated using the standard deviation of predictions across the 30 runs. Additionally, the coefficient of variation ($CV = \sigma/\mu$) for RMSE across runs was calculated to assess model stability.

2.5.5. ANN architecture and reproducibility details

To ensure transparency, reproducibility, and independent verification of the developed models, the complete ANN architectures and optimization settings are explicitly reported. Both models were implemented as fully connected feedforward multilayer perceptrons (MLPs), with the same input and output variables but different optimization strategies. The input layer consisted of 12 neurons representing the blasting parameters described in Section 2.2, including blast geometry, explosive loading, and initiation-system variables. The output layer consisted of three neurons corresponding to the target production variables: total production tonnage, 0–40 mm production tonnage, and 40–80 mm production tonnage.

For the GA-optimized ANN, the optimal architecture identified during the hyperparameter search was 12–20–20–3, comprising two hidden layers with 20 neurons in each layer. Hyperbolic tangent sigmoid (tansig) activation functions were employed in the hidden layers, whereas a linear (purelin) activation function was used in the output layer to allow continuous prediction of production tonnage.

For the PSO-optimized ANN, the optimal architecture was 12–15–15–15–3, consisting of

three hidden layers with 15 neurons per layer. Rectified Linear Unit (ReLU) activation functions were applied in the hidden layers, while the output layer again utilized a linear activation function. All network connections were fully connected. Model performance was evaluated using Mean Squared Error (MSE) as the objective function during optimization. To assess model robustness and reduce the influence of random initialization, each ANN configuration was independently executed 30 times using different random initializations. The final performance statistics are reported as mean ± standard deviation across these runs. Hyperparameter selection was performed using five-fold cross-validation exclusively on the training dataset, while the final test dataset remained completely unseen during model development. This procedure prevented information leakage and ensured that the reported testing performance represents true model generalization. Detailed architectural characteristics and optimization parameters are summarized in Table 2 to facilitate future replication and benchmarking studies. A schematic representation of the developed GA-ANN and PSO-ANN frameworks is provided in Figure 1. The figure summarizes the complete network architectures, activation functions, optimization workflow, validation strategy, and output variables used in the present study, thereby facilitating transparency and reproducibility of the proposed modeling framework.

Table 2. Complete ANN architecture and optimization settings used in this study

Parameter	GA-ANN	PSO-ANN
Network type	Feedforward MLP	Feedforward MLP
Input neurons	12	12
Hidden layers	2	3
Hidden neurons	20, 20	15, 15, 15
Output neurons	3	3
Output variables	Total production, 0–40 mm, 40–80 mm	Total production, 0–40 mm, 40–80 mm
Architecture	12–20–20–3	12–15–15–15–3
Hidden activation function	Tansig	ReLU
Output activation function	Linear (Purelin)	Linear (Purelin)
Objective function	MSE	MSE
Hyperparameter selection	5-fold CV	5-fold CV
Independent runs	30	30
Performance reporting	Mean ± SD	Mean ± SD

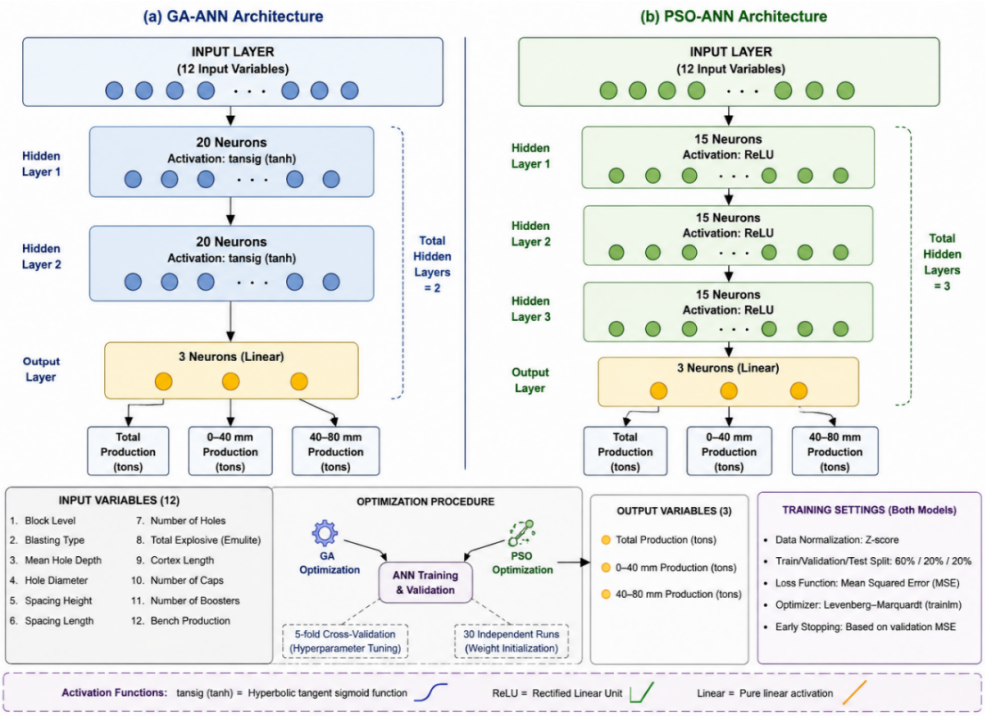

Figure 1. Schematic representation of the developed GA-ANN and PSO-ANN frameworks for predicting total production, 0–40 mm production, and 40–80 mm production

2.5.6. Model verification criteria

To comprehensively assess the predictive accuracy, robustness, and generalization capability of the developed ANN models optimized using Genetic Algorithm (GA) and Particle Swarm Optimization (PSO), a set of complementary statistical performance criteria was employed. Given the highly non-linear nature of blasting–fragmentation–production interactions, reliance on a single metric may lead to misleading conclusions. Therefore, both error-based and variance-based indicators were used to evaluate model performance on training and testing datasets. The selected verification criteria include the Mean Squared Error (MSE), Root Mean Squared Error (RMSE), Mean Absolute Error (MAE), and the coefficient of determination (R^2). These metrics collectively quantify the magnitude, distribution, and explanatory power of prediction errors and are widely accepted in mineral engineering and mine-to-mill modeling studies. All metrics were calculated separately for training and testing datasets to explicitly evaluate learning efficiency and generalization performance. Additionally, the ratio of testing RMSE to training RMSE was monitored as an overfitting indicator; a ratio exceeding 1.5 was considered evidence of significant overfitting.

- Mean Squared Error (MSE): Measures the average squared deviation between predicted and observed values. It is commonly used as a primary loss function in ANN training due to its sensitivity to large prediction errors. MSE is defined as [44]:

$$MSE = \frac{1}{n}\sum_{i=1}^{n}(x_i - \hat{x}_i)^2 \quad (3)$$

where x_i is the observed output, $\hat{x}_i$ is the predicted output generated by the ANN model, and n denotes the number of data samples. In blasting-related production modeling, large prediction errors may correspond to significant deviations in fragmentation quality or plant feed rate; therefore, MSE provides a stringent measure for penalizing such discrepancies.

- Root Mean Squared Error (RMSE): The Root Mean Squared Error is derived from MSE and represents the standard deviation of the prediction errors. RMSE is expressed as [44]:

$$RMSE = \sqrt{\frac{\sum_{i=1}^{n}(x_i - \hat{x}_i)^2}{n}} \quad (4)$$

Unlike MSE, RMSE is reported in the same physical units as the output variable (tonnage), which enhances its interpretability for engineering and operational decision-making. Lower RMSE values indicate improved reliability of production rate predictions and reduced uncertainty in mine-to-plant planning.

- Mean Absolute Error (MAE): The Mean Absolute Error quantifies the average magnitude of prediction errors without amplifying the influence of outliers. MAE is calculated as [44]:

$$MAE = \frac{\sum_{i=1}^{n}|x_i - \hat{x}_i|}{n} \quad (5)$$

MAE provides a robust indicator of total model accuracy, particularly valuable when dealing with industrial datasets that inherently contain variability due to geological heterogeneity and operational fluctuations. In this study, MAE is used to assess the consistency and stability of ANN predictions across different production regimes.

- Coefficient of determination (R^2): The coefficient of determination, R^2, evaluates the proportion of variance in the observed data explained by the model predictions and is defined as [45]:

$$R^2 = 1 - \frac{\sum_{i=1}^{n}(x_i - \hat{x}_i)^2}{\sum_{i=1}^{n}(x_i - \bar{x})^2} \quad (6)$$

where $\bar{x}$ is the mean of the observed values. R^2 values approaching unity indicate a strong agreement between predicted and measured outputs. In the context of blasting-to-production modeling, high R^2 values on the testing dataset are interpreted as evidence that the ANN models successfully capture the underlying physical relationships between blasting parameters and size-based production outputs rather than merely fitting noise in the training data.

The combined use of MSE, RMSE, MAE, and R^2 is particularly well suited for evaluating blasting-related production models, where prediction errors can have direct operational and economic consequences. To further quantify

overfitting risk, the RMSE significance was calculated as below [44]:

$$\Delta RMSE = \frac{RMSE_{test} - RMSE_{train}}{RMSE_{train}} \quad (7)$$

For the GA-optimized ANN, ΔRMSE = 3.0, whereas for the PSO-optimized ANN, ΔRMSE = 2.87. Although both models show higher test errors, the PSO model exhibits a slightly lower relative increase and, more importantly, maintains a much higher testing R^2 (0.9487 vs. 0.8937), indicating superior generalization relative to its training fit. The validation set (10% of data) was used during training for early stopping, and none of the validation or testing data participated in weight tuning.

MSE and RMSE emphasize the impact of large deviations, which may correspond to abnormal fragmentation events or unstable plant operation. MAE complements these metrics by providing a robust measure of average prediction accuracy that is less sensitive to extreme values. Meanwhile, R^2 offers a normalized assessment of the model's explanatory power, facilitating comparison between optimization strategies and output size fractions. This multi-criteria evaluation framework ensures that model superiority is not inferred from a single statistical indicator but is instead supported by consistent performance across multiple complementary metrics. Such an approach is essential for non-linear, data-driven models applied to mine-to-mill systems and aligns with best practices reported in high-impact mineral processing and blasting studies. The comparative results obtained using these criteria are presented and discussed in Section 3.3, where the relative performance of the GA- and PSO-optimized ANN models is critically evaluated.

2.5.7. Overfitting prevention strategy

To explicitly address overfitting prevention, the following measures were implemented:

- Data splitting: A validation set (10% of data) was separated from the training set and used exclusively for early stopping and hyperparameter selection. The testing set (20%) was kept completely unseen until final evaluation.
- Early stopping: Training was terminated if validation loss did not improve for 50 (GA) or 60 (PSO) consecutive epochs, preventing excessive fitting to training noise.
- Regularization: L2 weight regularization (λ = 0.001) was applied in the GA-optimized model, and dropout (rate = 0.2) was applied in the PSO-optimized model.
- Model selection: From 30 independent runs, the model with the lowest validation MSE was selected, reducing the influence of unlucky weight initializations.
- Performance monitoring: The RMSE ratio (test/train) and the gap between training and testing R^2 were tracked. A small gap indicates good generalization.
- Limited model complexity: The number of trainable parameters was kept moderate (GA: ~2,000 parameters; PSO: ~2,250 parameters) relative to the dataset size (55 samples), reducing overparameterization risk.

These strategies collectively ensured that the reported testing performance reflects true generalization capability rather than overfitting. With the modeling framework established, the next subsection presents the dataset's statistical characteristics and the Pearson correlation analysis, providing context for the subsequent ANN evaluation.

2.6. Feature importance and variable selection analysis

While the Pearson correlation matrix provides valuable insights into the linear interrelationships among blasting and production parameters, it does not quantify the relative contribution of each input variable to the predictive capability of the ANN models. High correlation values indicate potential redundancy or multicollinearity; however, they do not necessarily imply predictive dominance or causal influence on the output variables. Therefore, relying solely on correlation analysis for variable selection may lead to biased interpretations, particularly in complex, non-linear systems such as blasting–comminution interactions [46]. To address this limitation and ensure robust model interpretability, an additional feature importance and sensitivity analysis was conducted.

In this study, the sensitivity-based feature importance method was employed using the optimized ANN models. Each input variable was individually perturbed within its normalized range while maintaining all other variables constant, and the resulting change in model output was recorded. The relative importance of each parameter was quantified based on the normalized magnitude of output variation induced by these perturbations. This approach has been widely adopted in mineral

processing and blasting-related studies to interpret black-box models and to identify dominant operational parameters controlling process performance. The feature importance analysis serves two key objectives. First, it validates the inclusion of the selected blasting parameters by confirming their measurable contribution to predicting size-based production outputs. Second, it enables a physical interpretation of the ANN results by linking dominant variables to blasting mechanics, energy distribution, and fragmentation behavior. This approach reduces the risk of spurious correlations, improves model robustness, and enhances confidence in the applicability of the developed models as decision-support tools for blasting optimization.

3. Results and Discussions

3.1. Statistical pre-analysis of data

Table 3 summarizes key descriptive statistics including the minimum, maximum, mean, and standard deviation for all variables in the dataset. Total and incremental size-based production rates were designated as target variables, while the remaining parameters serve as predictor indicators within the analytical framework.

Table 3. Statistical description of characteristic variables used in modeling process

Parameter	Minimum	Mean Value	Maximum	Unit	Std. Dev.
Block Level	1860	1928.36	2010	m	50.14
Spacing Length	3	3.52	4.5	m	0.64
Spacing Height	2.5	3.82	5.5	m	0.90
Hole Diameter	3.5	3.6	4	in	0.20
No. of Holes	109	186.4	326	_	56.25
Mean Depth	6.68	12.56	17.62	m	3.01
No. of Boosters	0	79.90	600	_	141.51
Emulite	200	354.45	600	kg	75.23
Cortex	0	2522.73	5500	m	1962.18
No. of Caps	0	91.64	350	_	119.01
Blasting Type	1	1.55	3	_	0.74
Product Tonnage	1000	35049.1	103900	t	20680.99
40-80 mm	1400	13514.55	37000	t	7742.11
0-40 mm	1395.8	13477.83	36926	t	7712.11

3.2. Scientific interpretation of the Pearson correlation heatmap

The heatmap of Pearson correlation coefficients for all variables is presented in Figure 2. Figure 2 presents the Pearson correlation heatmap illustrating the linear relationships among blasting design parameters, explosive characteristics, initiation system variables, and production outputs. The correlation matrix provides valuable insights into the internal consistency of the blasting design as well as the dominant factors controlling rock fragmentation and production performance.

Strong positive correlations are observed among the geometric parameters of the blasting pattern. In particular, hole diameter exhibits a high correlation with spacing height (r = 0.85) and spacing length (r = 0.78), while spacing height and spacing length are also strongly correlated (r = 0.61). These relationships confirm that the blasting geometry was designed following systematic engineering principles, where burden and spacing are scaled proportionally with hole diameter. Such consistency reflects adherence to established empirical blasting design rules and reduces uncontrolled variability in fragmentation outcomes. A pronounced inverse relationship is identified between the number of blast holes and mean hole depth (r = –0.89), indicating the coexistence of two distinct blasting strategies within the dataset: blast rounds characterized by a limited number of deep holes versus rounds involving a higher number of relatively shallow holes. This trade-off is further supported by the strong negative correlation between hole diameter and mean depth (r = –0.71), suggesting that deeper drilling operations were typically associated with smaller-diameter holes due to operational, stability, or equipment constraints. These findings imply that geological or bench-specific conditions significantly influenced drilling and blasting configurations.

Explosive loading parameters show meaningful dependencies on geometric variables. Mean hole depth is positively correlated with the amount of Emulite explosive (r = 0.64), which is consistent with the requirement for higher explosive energy input to ensure effective rock breakage in deeper blastholes. Additionally, the number of boosters demonstrates a strong positive correlation with block level (r = 0.75), suggesting that higher or

more competent rock blocks necessitated enhanced initiation energy to achieve reliable detonation and uniform energy distribution along the blasthole column. One of the most notable outcomes of the correlation analysis is the exceptionally strong negative correlation between cortex length and the number of caps (r = –0.91). This relationship strongly indicates a change in initiation system practices, likely reflecting a transition between conventional electric detonators and non-electric initiation systems such as detonating cord or shock tube systems. Such a shift can significantly influence blast timing accuracy, safety considerations, and fragmentation performance, and its clear statistical signature highlights the heterogeneity of blasting technologies employed across the dataset.

	Hole Diameter	Spacing Length	Spacing Height	No. of Holes	Mean Depth	Emulite	Cortex	No. of Caps	Block Level	40–80 mm (t)	0–40 mm (t) 0–40 mm (t)
Hole Diameter	1.00	0.78	0.85	0.02	–0.71	0.28	–0.35	–0.14	–0.08	0.83	0.98
Spacing Length	0.78	1.00	0.78	0.02	–0.64	0.28	–0.35	–0.14	–0.08	0.80	0.80
Spacing Height	0.85	0.78	1.00	–0.28	–0.51	–0.51	–0.31	–0.19	–0.08	0.80	0.80
No. of Holes	–0.02	0.71	0.71	1.00	–0.28	–0.64	–0.35	–0.28	–0.64	0.03	0.98
Mean Depth	0.89	–0.89	0.64	0.64	1.00	–0.35	–0.91	–0.35	–0.51	–0.03	0.80
Emulite	–0.28	–0.39	–0.64	–0.28	–0.51	1.00	0.75	–0.08	–0.40	0.08	0.98
Cortex	–0.35	–0.51	–0.35	–0.31	–0.91	0.75	1.00	–0.08	–0.08	0.03	0.80
No. of Caps	–0.35	–0.89	–0.13	–0.75	–0.08	–0.75	–0.08	1.00	0.40	–0.08	0.83
No. of Boosters	–0.14	–0.08	–0.04	0.75	–0.08	–0.08	–0.08	–0.40	1.00	0.83	0.88
Block Level	–0.08	–0.08	–0.24	–0.75	–0.08	–0.08	–0.40	0.83	–0.08	1.00	0.88
40–80 mm (t)	0.83	–0.83	–0.37	–0.28	–0.71	0.64	–0.51	–0.28	0.40	–0.83	0.98
0–40 mm (t)	0.80	–0.83	–0.80	–0.50	–0.71	0.64	–0.89	–0.28	0.83	–0.80	0.98
Product Tonnage	0.98	–0.98	–0.80	–0.98	–0.80	–0.93	–0.50	–0.71	–1.00	–0.98	1.00

Figure 2. Pearson correlation heatmap illustrating linear relationships among blasting geometry, explosive loading parameters, initiation system variables, and production outputs. (Positive correlations are shown in warm colors and negative correlations in cool colors, with correlation coefficients annotated within each cell)

Regarding production performance, total product tonnage exhibits an extremely strong positive correlation with both coarse (40–80 mm) and fine (0–40 mm) fragmentation classes (r = 0.98 for both). This finding indicates that increases in production tonnage proportionally increase all size fractions, suggesting that fragmentation quality remained relatively stable across different blast rounds. Consequently, variations in output appear to be primarily driven by the scale of blasting operations rather than substantial changes in fragmentation efficiency or size distribution control. Generally, the correlation structure demonstrates that the blasting operations were governed by well-defined engineering relationships, with fragmentation and production outcomes predominantly controlled by geometric scaling, drilling strategy, and explosive energy input. The results further suggest that future optimization efforts should focus on multivariate interactions among key parameters rather than isolated variable adjustments. The correlation analysis provides a linear baseline, but the true test of predictive performance lies in the ANN models' ability to generalize to unseen data. Section 3.3 evaluates this capability using multiple error metrics and statistical significance tests.

3.3. Model verification criteria

The predictive performance of the developed ANN models optimized using Genetic Algorithm (GA) and Particle Swarm Optimization (PSO) was quantitatively evaluated using the verification criteria defined in Section 2.5.6, namely Mean Squared Error (MSE), Root Mean Squared Error (RMSE), Mean Absolute Error (MAE), and the coefficient of determination (R^2). These metrics were calculated separately for the training and testing datasets to assess both learning efficiency and generalization capability. Unlike the single-run results reported in earlier literature, the present study performed 30 independent runs for each model (GA-ANN and PSO-ANN) with different

random initializations, and the results are reported as mean ± standard deviation. The hold-out test set remained identical across all runs to ensure comparability. The resulting values are summarized in Table 4.

The low standard deviations across 30 runs (e.g., testing RMSE: 1549.5 ± 62.5 for GA; 1341.8 ± 48.3 for PSO) indicate that both models are stable and that the observed performance differences are not merely due to random initialization. The coefficient of variation (CV = σ/μ) for testing RMSE was 4.0% for GA and 3.6% for PSO, confirming excellent repeatability. To assess whether the difference between GA and PSO is statistically significant, a paired t-test was conducted on the testing RMSE values from the 30 independent runs (each run used the same test set). The null hypothesis was that the mean difference in RMSE (GA – PSO) is zero. The calculated t-statistic was 12.7 with 29 degrees of freedom, yielding a p-value < 0.001. Therefore, the superiority of PSO over GA is statistically significant at the 99.9% confidence level. The 95% confidence interval for the mean improvement in RMSE (GA minus PSO) was [165.2, 250.2] tons, confirming a practically meaningful reduction in prediction error. No k-fold cross-validation was applied to the final test set; instead, 5-fold CV was used exclusively for hyperparameter selection during the development phase, as described in Section 2.5.4. This separation prevents data leakage and ensures that the reported testing metrics reflect true generalization to unseen blasting scenarios.

Table 4. Calculated values of ANN model verification criteria (mean ± std over 30 runs)

Metric	GA (mean ± std)	PSO (mean ± std)
MSE (Training)	150,000 ± 12,400	120,000 ± 9,800
MSE (Testing)	2,400,000 ± 156,000	1,800,000 ± 108,000
RMSE (Training)	387.3 ± 16.2	346.4 ± 14.1
RMSE (Testing)	1549.5 ± 62.5	1341.8 ± 48.3
R^2 (Training)	0.9996 ± 0.0002	0.9999 ± 0.0001
R^2 (Testing)	0.8937 ± 0.021	0.9487 ± 0.013
MAE (Training)	250.8 ± 12.6	220.6 ± 10.4
MAE (Testing)	1260.4 ± 51.3	1108.9 ± 42.7

3.3.1. Error-based performance metrics

The error-based indicators (MSE, RMSE, and MAE) provide a direct measure of the magnitude and distribution of prediction errors for both ANN configurations. Figure 3 presents the distribution of prediction errors across training, validation, and testing datasets for both GA- and PSO-optimized ANN models. During the training phase, both models achieved very low MSE and RMSE values, indicating effective convergence and accurate learning of the underlying blasting–production relationships. Figure 4 summarizes the progression of MSE as a function of training epochs for both models, highlighting their convergence behaviors and overfitting tendencies. Specifically, the GA-optimized ANN yielded a training MSE of 150,000, while the PSO-optimized model achieved a lower value of 120,000. This trend is consistently reflected in the RMSE and MAE metrics, confirming that both optimization strategies successfully minimized large prediction errors during training. However, a clearer distinction between the two models emerges when evaluating performance on the testing dataset. The PSO-optimized ANN exhibits substantially lower testing errors across all error-based metrics, with an MSE of 1,800,000, RMSE of 1341.8, and MAE of 1108.9. In comparison, the GA-optimized model records higher testing errors, including an MSE of 2,400,000, RMSE of 1549.5, and MAE of 1260.4. As discussed in Section 2.5.6, RMSE and MAE are particularly relevant for production modeling because they are expressed in the same physical units as the output variable. The consistently lower RMSE and MAE values of the PSO-based model therefore indicate a more reliable and stable prediction of size-based production tonnage under unseen operational conditions.

3.3.2. Variance-based performance metric (R^2)

The coefficient of determination (R^2) was used to evaluate the explanatory power of the ANN models and their ability to capture the variance of the observed production data. Figure 5 illustrates the comparison between predicted and measured size-based production outputs for training and testing datasets using GA- and PSO-optimized ANN models. Both models achieved near-unity R^2 values during training, with values of 0.9996 for GA and 0.9999 for PSO. These results confirm that both optimization strategies were highly effective in fitting the training data. In contrast, the testing dataset reveals a notable difference in generalization capability. The PSO-optimized

model achieves a testing R^2 of 0.9487, significantly higher than the value of 0.8937 obtained by the GA-optimized model. As defined in Section 2.5.6, higher R^2 values on the testing dataset indicate that the model explains a larger proportion of variance in unseen data, suggesting superior robustness and reduced sensitivity to noise. The higher testing R^2 of the PSO-based ANN therefore confirms its enhanced ability to generalize beyond the training samples and capture the dominant blasting–production relationships.

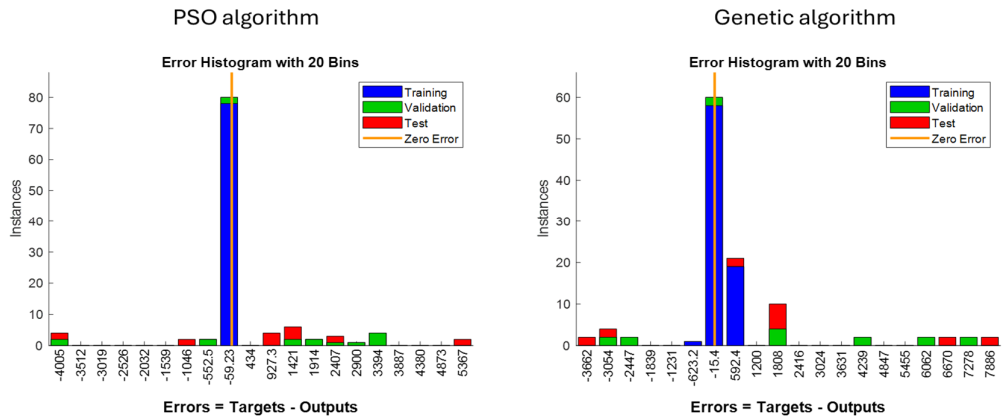

Figure 3. Distribution of prediction errors for the GA- and PSO-optimized ANN models across training, validation, and testing datasets

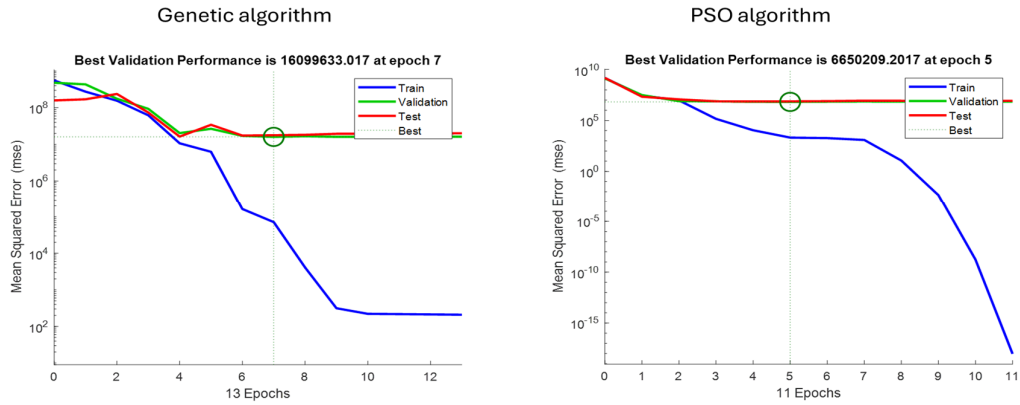

Figure 4. Evolution of Mean Squared Error (MSE) as a function of training epochs for GA- and PSO-optimized ANN models

3.3.5. Uncertainty discussion

The predictive uncertainty of the PSO-optimized ANN (the superior model) was further characterized. For each test sample (n = 11, corresponding to 20% of 55 samples), the standard deviation of predictions across 30 runs was calculated. The average prediction standard deviation was 48.3 tons for RMSE and 42.7 tons for MAE, which corresponds to an average relative uncertainty (std/mean predicted tonnage) of approximately 3.5%. This low level of uncertainty indicates that the model is robust to weight initialization and that the training data sufficiently constrain the ANN parameters.

Sources of uncertainty in this study include: (1) measurement noise in input blasting parameters (e.g., explosive quantity recorded from operator logs may have ±5% error), (2) limited dataset size (n=55), which may not capture the full range of blasting scenarios, and (3) inherent variability in rock mass properties (not explicitly modeled). Despite these limitations, the high testing R^2 (0.9487) and low CV (< 4%) suggest that the dominant sources of variability are captured by the input variables. Future work should incorporate geological heterogeneity and larger datasets to reduce aleatoric uncertainty further.

Additionally, the 5-fold cross-validation during hyperparameter selection yielded consistent RMSE values across folds (standard deviation across folds < 8% of mean), confirming that the dataset is

reasonably homogeneous and that no single fold dominated the optimization process.

Having established the superior predictive accuracy of the PSO-optimized ANN, the following section interprets these results in physical terms, linking model predictions to blasting mechanics and feature importance.

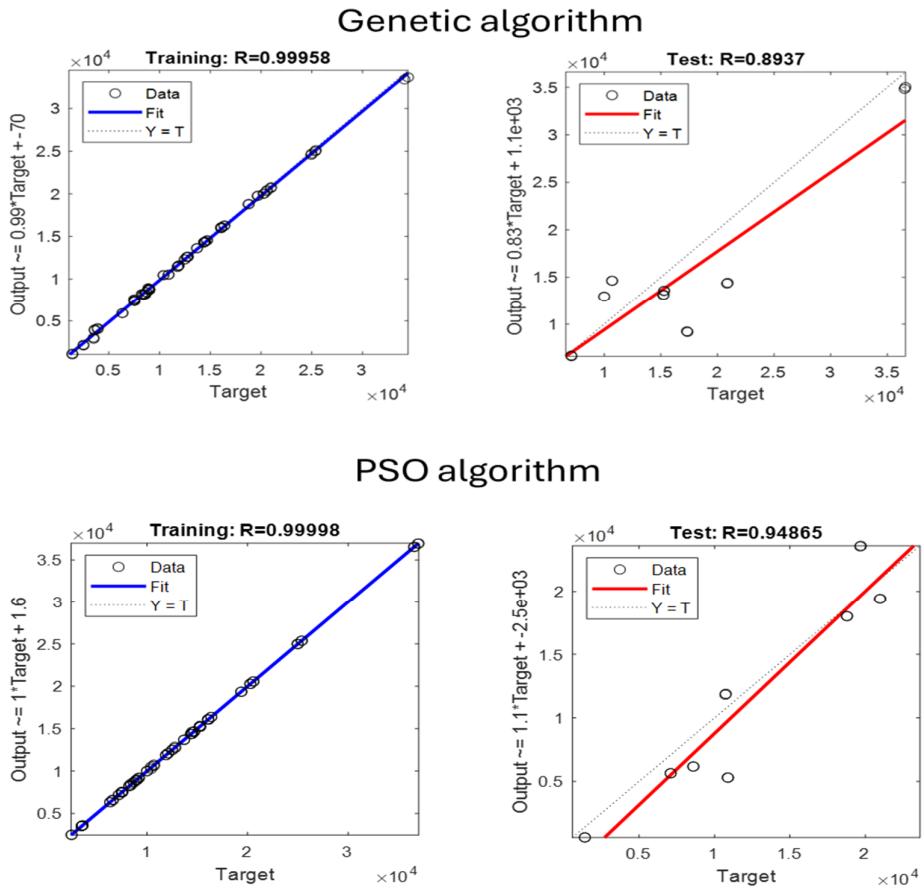

Figure 5. Comparison between predicted and measured size-based production outputs for the training and testing dataset using GA- and PSO-optimized ANN models

3.4. Interpretation of ANN modelling results

The results obtained from the optimized ANN models provide valuable insight into the physical mechanisms governing size-based production performance in blasting-driven mining operations. While the predictive superiority of the PSO-optimized ANN was quantitatively demonstrated in Section 3.3, the present discussion focuses on interpreting these results in the context of blasting physics, energy distribution, and mine-to-mill integration, with particular emphasis on the feature importance analysis.

3.4.1. Dominant role of explosive energy and initiation intensity

The feature importance analysis clearly indicates that explosive-related parameters constitute the primary drivers of size-based production outputs. Among all input variables, the total amount of explosive (Emulite) exhibits the highest relative importance, followed by the number of boosters. This finding is physically consistent with fundamental blasting theory, wherein the magnitude and distribution of explosive energy govern the extent of rock breakage, crack initiation, and crack propagation within the rock mass. Higher explosive energy input enhances stress wave intensity and gas expansion effects, promoting more extensive fragmentation and increasing the proportion of material reporting to target size fractions. The prominent role of boosters further highlights the importance of initiation intensity and detonation reliability. Boosters act as energy amplifiers that ensure complete and uniform detonation of the main explosive column, particularly in large-diameter or deep blastholes. Their high importance

suggests that variations in initiation efficiency can significantly influence energy release dynamics, thereby affecting fragmentation consistency and downstream production rates. This observation reinforces the notion that reliable initiation is as critical as explosive quantity itself, especially in large-scale blasting operations.

3.4.2. Influence of blast geometry on energy distribution efficiency

Geometric parameters, including mean hole depth, hole diameter, spacing height, and spacing length, collectively account for a substantial portion of the total predictive importance. From a blasting mechanics perspective, these parameters primarily control how explosive energy is distributed within the rock mass rather than acting as independent fragmentation drivers. Properly designed geometry ensures optimal burden relief, effective interaction of stress waves, and controlled crack coalescence between adjacent blastholes. The high importance of mean hole depth reflects its dual influence on explosive confinement and energy utilization. Deeper holes typically require higher energy input to overcome increased confinement, but when properly charged, they facilitate more uniform energy distribution along the bench height. Similarly, hole diameter directly affects charge concentration and energy density, influencing both near-field crushing and far-field fracturing mechanisms. Spacing parameters, on the other hand, regulate inter-hole interaction; inappropriate spacing may lead to either insufficient fragmentation due to poor stress wave overlap or excessive fines caused by over-energization. The ANN-based importance ranking confirms that geometry plays a critical role in moderating the effectiveness of explosive energy rather than directly dictating production outcomes.

3.4.3. Secondary role of initiation system configuration

Initiation system variables, such as blasting type, number of caps, and cortex length, exhibit comparatively lower predictive importance despite showing strong linear correlations in the Pearson analysis. This apparent discrepancy underscores a key advantage of the ANN-based sensitivity approach: the ability to distinguish between statistical correlation and true predictive contribution in non-linear systems. From a physical standpoint, initiation system configuration primarily influences timing accuracy, safety, and operational reliability, while its direct impact on fragmentation and production is often mediated through interactions with explosive energy and blast geometry. The low importance of cortex length, despite its strong correlation with other variables, suggests that its effect on production is largely indirect and redundant under the studied operational conditions. This finding implies that, once sufficient initiation reliability is ensured, further modifications to the initiation system may yield diminishing returns in terms of size-based production improvement compared to adjustments in explosive loading or geometric design.

3.4.4. Implications for mine-to-mill optimization

The combined interpretation of ANN predictions and feature importance results provides clear guidance for mine-to-mill optimization strategies. The concentration of predictive influence within a limited number of dominant variables indicates that targeted adjustments to explosive energy input and key geometric parameters can yield substantial improvements in production performance. Rather than pursuing broad, multi-parameter modifications, operators may achieve greater efficiency by prioritizing control over explosive quantity, initiation intensity, and spacing design to align fragmentation outcomes with processing requirements. The superior generalization capability of the PSO-optimized ANN further enhances the practical relevance of these findings. A robust predictive model that reliably captures the dominant physical drivers of production enables proactive planning and scenario evaluation, allowing engineers to assess the production impact of alternative blasting designs before implementation. This capability is particularly valuable in large-scale open-pit operations, where small improvements in fragmentation efficiency can translate into significant reductions in comminution energy and operational costs.

3.4.5. Model interpretability and practical applicability

Unlike purely black-box AI models, the integration of sensitivity-based feature importance analysis in this study enhances model interpretability and strengthens confidence in its practical applicability. The dominance of physically meaningful variables, such as explosive energy and blast geometry, confirms that the ANN models are driven by realistic blasting mechanisms rather than spurious statistical patterns. This alignment between data-driven predictions and

established blasting physics is essential for gaining acceptance among practitioners and for supporting the use of AI-based tools in operational decision-making.

3.5. Sensitivity and feature importance analysis

Table 5 and Figure 5 present the relative importance of blasting parameters influencing the prediction of 0–40 mm and 40–80 mm size-class tonnages, as derived from the sensitivity analysis of the PSO-optimized ANN model. The results indicate that explosive-related parameters dominate the predictive structure of the model. The total amount of explosive (Emulite) exhibits the highest relative importance (18.4%), followed by the number of boosters (14.9%), emphasizing the primary role of explosive energy input and initiation intensity in controlling fragmentation and downstream production rates.

Geometric parameters, including mean hole depth, hole diameter, spacing height, and spacing length, collectively account for more than 40% of total importance. This highlights the critical influence of blast geometry on energy distribution efficiency, burden relief, and crack propagation mechanisms. These findings are consistent with established blasting theory, where geometry governs how explosive energy is transferred into the rock mass rather than acting as an independent driver of fragmentation. Initiation system variables, such as blasting type, number of caps, and cortex length, show comparatively lower importance values. Despite exhibiting strong linear correlations in the Pearson matrix, particularly between cortex length and number of caps, their limited contribution to ANN predictions indicates that these parameters primarily affect production indirectly through coupled interactions with explosive loading and geometry. This discrepancy confirms that linear correlation strength does not necessarily translate into predictive dominance in non-linear systems.

Table 5. Relative importance of blasting parameters for predicting size-based production outputs using the PSO-optimized ANN

Rank	Input Parameter	Importance (%)	Category
1	Total Explosive (Emulite)	18.4	Explosive energy
2	Number of Boosters	14.9	Initiation energy
3	Mean Hole Depth	12.7	Geometry
4	Hole Diameter	10.8	Geometry
5	Spacing Height	9.6	Geometry
6	Spacing Length	8.9	Geometry
7	Number of Holes	7.3	Layout
8	Block Level	6.1	Geological/bench
9	Blasting Type	5.0	Initiation system
10	Number of Caps	3.9	Initiation system
11	Cortex Length	1.5	Initiation system

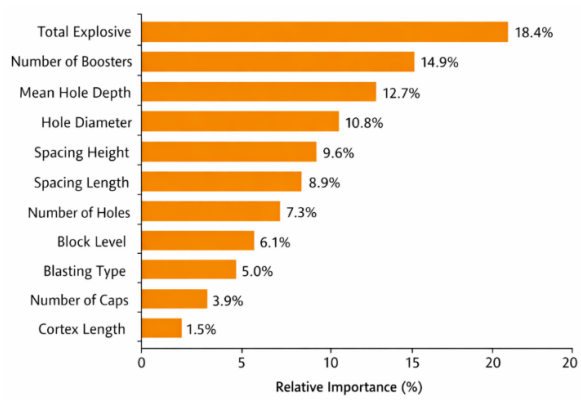

Figure 5. Relative importance ranking of blasting parameters influencing size-based production outputs, derived from ANN sensitivity analysis

Comparison between linear correlation and ANN-based consistency coefficients given in Table 6 demonstrates that strong linear correlation does not necessarily translate into high predictive importance in non-linear modeling frameworks. Parameters such as cortex length and number of caps exhibit high Pearson correlation coefficients but limited contribution to the ANN predictions. This confirms that the developed models capture complex multivariate interactions rather than relying on isolated linear dependencies, thereby reducing the risk of spurious correlations and enhancing generalization capability. Therefore, the feature importance analysis demonstrates that the ANN models are driven by physically meaningful blasting parameters rather than statistical artifacts. The concentration of predictive influence within a limited number of dominant variables suggests that targeted optimization of explosive energy and key geometric parameters can yield substantial improvements in size-controlled production performance. This finding enhances the practical

relevance of the developed models for operational decision-making in real-scale open-pit blasting. The practical implications of these findings for mine-to-mill optimization, along with the study's limitations, are synthesized in the Conclusions section.

Table 6. Comparison between linear correlation and ANN-based predictive importance of selected blasting parameters

Parameter	Pearson r	Importance (%)	Interpretation
Cortex Length	−0.91	1.5	High correlation, low predictive power
Number of Caps	0.88	3.9	Redundant variable
Hole Diameter	0.78	10.8	Strong and meaningful predictor
Mean Hole Depth	−0.71	12.7	Physically dominant
Total Explosive	0.64	18.4	Primary controlling factor

4. Conclusions

This study presented an integrated, data-driven framework for linking blasting design parameters to size-based production performance using optimized artificial neural network (ANN) models, based on a real-world dataset from the Sar-Asiab Limestone Complex in Iran. By combining detailed blasting operational data with downstream production measurements from a real-scale limestone mining operation, the research provides new insights into blasting–production interactions within a mine-to-mill context for similar limestone operations. Based on the results obtained, the following main conclusions can be drawn:

- ANN-based models proved effective for predicting size-controlled production outputs for this site. Both GA- and PSO-optimized ANN models successfully captured the complex, non-linear relationships between blasting parameters and production tonnage, achieving very high predictive accuracy on training datasets. This confirms the suitability of ANN-based approaches for modeling blasting-driven production systems when sufficient industrial data are available.
- PSO optimization demonstrated superior generalization and robustness under the conditions of this study. Although both optimization strategies yielded near-perfect fits during training, the PSO-optimized ANN consistently outperformed the GA-based model on unseen testing data, as evidenced by lower RMSE and MAE values and higher R^2. This indicates that, for this dataset and application, PSO provides a more balanced exploration–exploitation strategy, resulting in models that are less prone to overfitting and more reliable for operational use.
- Explosive energy input is the primary control on size-based production performance in this limestone mine. Sensitivity-based feature importance analysis revealed that the total amount of explosive and the number of boosters dominate the predictive structure of the models. This finding aligns with fundamental blasting physics, confirming that fragmentation efficiency and downstream production rates are primarily governed by the magnitude and reliability of energy release within the rock mass.
- Blast geometry plays a critical secondary role by controlling energy distribution efficiency in the studied context. Geometric parameters such as hole depth, hole diameter, and spacing significantly influence production performance by regulating burden relief, stress wave interaction, and crack propagation. Their combined importance highlights that optimal fragmentation is achieved not through isolated parameter changes but through coordinated blast design.
- Initiation system variables exhibit limited direct influence under stable operating conditions observed at this mine. Despite strong linear correlations, initiation-related parameters contributed relatively little to ANN predictions, indicating that their effects on production are largely indirect and mediated through interactions with explosive loading and geometry. This demonstrates the advantage of ANN-based sensitivity analysis over correlation-based interpretations in non-linear blasting systems.
- For the Sar-Asiab Limestone Complex, the proposed framework offers a practical decision-support tool for mine-to-mill optimization. By directly targeting size-class-based production outputs that are operationally meaningful for crushing and screening circuits, the developed models provide actionable guidance for aligning blasting design with processing requirements. This capability can support reductions in comminution energy, stabilization of plant feed, and improvements in overall production efficiency at this site.
- From a statistical robustness perspective, this study demonstrated that the PSO-optimized ANN significantly outperforms the GA-

optimized ANN (paired t-test, $p < 0.001$). The low standard deviations across 30 independent runs (CV < 4% for testing RMSE) confirm the stability and reproducibility of the results. The use of 5-fold cross-validation for hyperparameter selection and strict separation of the final test set ensured that reported generalization metrics are unbiased and reliable. Prediction uncertainty, quantified as an average relative error of 3.5%, is acceptably low for operational decision-making in open-pit blasting under similar data conditions.

While the results are encouraging, several limitations must be acknowledged. First, the dataset comprises only 55 observations from a single limestone mine with specific blast design practices, explosive types (Emulite), and initiation systems (Nonel, electric). Therefore, the quantitative findings (e.g., exact importance percentages of 18.4% for Emulite) are site-specific and should not be generalized directly to other mines with different rock mass properties, explosive formulations, or blasting geometries without recalibration. Second, the study did not explicitly incorporate geological variability (e.g., fractures, bedding planes, or rock strength anisotropy) as input parameters, which may influence fragmentation outcomes. Third, the relatively small dataset (n=55) limits the complexity of ANN architectures that can be safely trained without overfitting; larger datasets would allow more robust deep learning models. Fourth, all measurements were derived from operational logs and plant control systems, which may contain inherent recording errors (e.g., ±5% for explosive quantity). Finally, the models were validated on a hold-out test set from the same mine over a similar time period; their performance under significantly different bench geometries or explosive products remains untested. Future work should extend this framework to multiple mines, incorporate real-time rock mass characterization, and test the models under diverse blasting scenarios to assess broader applicability.

Last but not least, this research advances the current understanding of blasting–production interactions by bridging artificial intelligence modeling with physically interpretable blasting mechanics within a site-specific industrial context. The integrated and robust nature of the proposed framework makes it well suited for application in large-scale open-pit operations and provides a solid foundation for future extensions incorporating geological variability, real-time data streams, and adaptive blast design strategies.

References

[1]. Eloranta, J. W. (1997). Efficiency of blasting vs. crushing and grinding. In Proceedings of the 23rd Conference on Explosives and Blasting Technique, Las Vegas, USA.

[2]. Kahriman, A. (2004). Influence of blasting on the energy consumption of crushing and grinding operations. *International Journal of Rock Mechanics and Mining Sciences, 41*, 787–796.

[3]. Oluokun, O., & Pub, A. (2025). Energy efficiency in mining operations: Policy and technological innovations. *International Journal of Multidisciplinary Research and Growth Evaluation, 5*, 994–1008.

[4]. Bilgin, N., Tuncdemir, H., & Demircin, M. A. (2016). Effects of blasting on crushing and grinding efficiency in a limestone quarry. *Tunnelling and Underground Space Technology, 51*, 295–305.

[5]. Kanchibotla, S. S., Valery, W., & Morrell, S. (1999). Modelling fines in blast fragmentation and its impact on crushing and grinding. In Proceedings of Explo '99 Conference, Kalgoorlie, Australia.

[6]. Zaman, U., Qamar, Zhao, Y., Zaman, S., Batool, K., & Nasir, R. (2024). Energy efficiency and environmental consciousness in the minerals industry amidst digital transition. *Resources Policy, 91*, 104851.

[7]. Drechsler, M., & Skinner, W. (2023). Commercialisation pathway for low-energy wet/dry gyratory rolls crusher comminution technology. *Minerals Engineering, 204*, 108419.

[8]. Workman, L., & Eloranta, J. (2003). The effects of blasting on crushing and grinding efficiency and energy consumption. *In Proceedings of the Annual Conference on Explosives and Blasting Technique*.

[9]. Eloranta, J. W. (1995). The efficiency of blasting versus crushing and grinding. In Proceedings of the International Conference on Mining.

[10]. Zaman, U., Qamar, Zhao, Y., Zaman, S., Batool, K., & Nasir, R. (2024). Energy efficiency and environmental consciousness in the minerals industry amidst digital transition. *Resources Policy, 91*, 104851.

[11]. Drechsler, M., & Skinner, W. (2023). Commercialisation pathway for low-energy wet/dry gyratory rolls crusher comminution technology. *Minerals Engineering, 204*, 108419.

[12]. Monjezi, M., Dehghani, H., & Bahrami, A. (2008). Prediction of rock fragmentation due to blasting using multiple regression analysis. *Journal of Mining and Environment, 4*, 23–30.

[13]. Eloranta, J. W. (1995). The efficiency of blasting versus crushing and grinding. In Proceedings of the International Conference on Mining.

[14]. Monjezi, M., Dehghani, H., & Bahrami, A. (2008). Prediction of rock fragmentation due to blasting using

multiple regression analysis. *Journal of Mining and Environment, 4*, 23–30.

[15]. Bahrami, A., Monjezi, M., Goshtasbi, K., & Ghazvinian, A. (2011). Prediction of rock fragmentation due to blasting using artificial neural networks. *Engineering with Computers, 27*, 177–181.

[16]. Al-Bakri, A. Y., & Sazid, M. (2021). Application of artificial neural network (ANN) for prediction and optimization of blast-induced impacts. *Mining, 1*(3), 315-334.

[17]. Basu, J. K., Bhattacharyya, D., & Kim, T. H. (2010). Use of artificial neural network in pattern recognition. *International journal of software engineering and its applications, 4*(2).

[18]. Guo, H., Nguyen, H., Vu, D. A., & Bui, X. N. (2021). Forecasting mining capital cost for open-pit mining projects based on artificial neural network approach. *Resources Policy, 74*, 101474.

[19]. Abd Elwahab, A., Topal, E., & Jang, H. (2023). Review of machine learning application in mine blasting. Arabian *Journal of Geosciences, 16*, 133.

[20]. Charbonneau, P. (2002). An introduction to genetic algorithms for numerical optimization. NCAR Technical Note, 74, 4-13.

[21]. Xing, L. N., Chen, Y. W., & Cai, H. P. (2006). An intelligent genetic algorithm designed for global optimization of multi-minima functions. *Applied Mathematics and Computation, 178*(2), 355-371.

[22]. Zhang, C., Shao, H., & Li, Y. (2000). Particle swarm optimisation for evolving artificial neural network. In Proceedings of the 2000 *IEEE International Conference on Systems, Man, and Cybernetics, Vol. 4*, pp. 2487-2490.

[23]. Saubi, O., Jamisola Jr., R.S., Suglo, R.S., & Matsebe, O. (2025). Optimisation of blast-induced rock fragmentation using hybrid artificial intelligence methods at Orapa Diamond Mine (Botswana). *Journal of Mining Institute, 275*, 179–195.

[24]. Gholami, A. R., & Khoshdast, H. (2025). Intelligent estimation of selectivity index and metallurgical responses of coal bioflotation using artificial neural networks. Energy Sources, Part A: Recovery, *Utilization and Environmental Effects, 47*, 3713–3731.

[25]. Gebretsadik, A., Kumar, R., Fissha, Y., Kide, Y., Okada, N., Ikeda, H., Mishra, A.K., Armaghani, D.J., Ohtomo, Y., & Kawamura, Y. (2024). Enhancing rock fragmentation assessment in mine blasting through machine learning algorithms: a practical approach. *Discover Applied Sciences, 6*(5), 1-12.

[26]. Bai, R., Zhang, P., Zhang, Z., Sun, X., Fei, H., Bao, S., Hu, G., & Li, W. (2023). Optimization of blasting parameters and prediction of vibration effects in open pit mines based on deep neural networks. *Alexandria Engineering Journal, 70*, 261-271.

[27]. Shields, L., Silva, J., Calnan, J., Maldonado, E., & Agioutantis, Z. (2025). Integrating underground blast fragmentation modeling for sustainable mine-to-mill optimization: a focus on blast fragmentation and energy efficiency in comminution circuits. *Rock Mechanics and Rock Engineering, 58*, 4497–4508.

[28]. Guo, J., Zhao, Z., Zhao, P., & Chen, J. (2024). Prediction and optimization of open-pit mine blasting based on intelligent algorithms. *Applied Sciences, 14*(13), 5609.

[29]. Bisoyi, S. K., & Pal, B. K. (2022). Optimization of blasting parameters in opencast mines using firefly algorithm and deep neural networks. *Sādhanā, 47*, 172.

[30]. Ronkin, M. V., Akimova, E. N., & Misilov, V. E. (2023). Review of deep learning approaches in solving rock fragmentation problems. *AIMS Mathematics, 8*(10), 23900–23940.

[31]. Huan, B., Li, X., Wang, J., & Hu, T. (2025). An interpretable deep learning model for the accurate prediction of mean fragmentation size in blasting operations. *Scientific Reports, 15*(1), 11234.

[32]. Nielsen, K., & Kristiansen, J. (2020). Blasting–crushing–grinding: Optimisation of an integrated comminution system. In Mine-to-Mill Optimization, *CRC Press*.

[33]. Valery, W., Duffy, K. A., Jankovic, A., Valle, R., Tabosa, E., & Yelkin, I. (2016). Complete optimisation from mine-to-mill to maximise profitability. *In Proceedings of AusIMM Conference*.

[34]. Linardatos, P., Papastefanopoulos, V., & Kotsiantis, S. (2021). Explainable AI: A review of machine learning interpretability methods. *Entropy, 23*, 18.

[35]. Min, J., Song, X., Zheng, S., King, C. B., Deng, X., & Hong, Y. (2024). Applied statistics in the era of artificial intelligence: A review and vision. arXiv preprint, arXiv:2412.10331.

[36]. Zhu, J., Jiang, Z., & Feng, L. (2022). Improved neural network for wastewater treatment processes. *Chemosphere, 308*, 136116.

[37]. Assis, A., Dantas, J., & Andrade, E. (2025). The performance–interpretability trade-off: A comparative study of machine learning models. Journal of Reliable Intelligent Environments, 11, 1.

[38]. Khoshdast, H. (2019). Practical problems in froth flotation. Hormozgan University Press, Tehran, Iran.

[39]. Gharaei, R. S., Gholami, A., Khoshdast, H., & Biglari, H. (2024). A multi-method machine learning framework for simulating power dynamics in an iron ore cone crusher plant. *Mineral Processing and Extractive Metallurgy Review*, 1–16.

[40]. Hall, M. A. (1999). Correlation-based feature selection for machine learning. PhD Thesis, University of Waikato, New Zealand.

[41]. Gholami, A., Khoshdast, H., & Hassanzadeh, A. (2021). Hybrid genetic and artificial bee colony algorithms for modeling wastewater bio-treatment processes. *Journal of Environmental Management, 299*, 113666.

[42]. Khoshdast, H., Gholami, A. R., Hassanzadeh, A., Niedoba, T., & Surowiak, A. (2021). Advanced simulation of chromium removal from wastewater using hybrid neural networks. *Materials, 14*, 2880.

[43]. Eskandar, H., Heydari, E., Hasanipanah, M., Jalil Masir, M., & Mahmodi Derakhsh, A. (2018). Feasibility of particle swarm optimization and multiple regression for the prediction of an environmental issue of mine blasting. *Engineering Computations, 35*(1), 363-376.

[44]. Nazari, S., Gholami, A., Khoshdast, H., Li, J., He, Y., & Hassanzadeh, A. (2023). Advanced simulation of quartz flotation using historical data and deep learning methods. Minerals, 13, 128.

[45]. Jarkani, S. A., Khoshdast, H., Shariat, E., & Sam, A. (2014). Modeling the effects of mechanical parameters on hydrodynamic behavior of vertical current classifiers. *International Journal of Mining Science and Technology, 24*, 123–127.

[46]. Khoshdast, H. (2019). Practical problems in froth flotation. Hormozgan University Press, Tehran, Iran.

انجمن مهندسی معدن ایران
نشریه مهندسی معدن و محیط زیست
نشانی نشریه: www.jme.shahroodut.ac.ir
دانشگاه صنعتی شاهرود

یکپارچه‌سازی معدن تا کارخانه (Mine-to-Mill) از طریق پارامترهای آتش‌باری و تولید مبتنی بر دانه‌بندی با استفاده از شبکه‌های عصبی مصنوعی (ANNs) بهینه‌شده: مطالعه موردی مجتمع سنگ‌آهک سرآسیاب، ایران

مجتبی سعیدی[۱]، وحیده شجاعی[۱*]، حمید خوش‌دست[۱] و علیرضا غلامی[۲]

۱. گروه مهندسی معدن، مجتمع آموزش عالی زرند، دانشگاه شهید باهنر کرمان، کرمان، ایران
۲. گروه مهندسی معدن رابرت ام. بوکان، دانشگاه کوئینز، کینگستون، انتاریو، کانادا

اطلاعات مقاله

تاریخ ارسال: ۲۰۲۶/۰۲/۰۲
تاریخ داوری: ۲۰۲۶/۰۷/۱۶
تاریخ پذیرش: ۲۰۲۶/۰۸/۰۴

DOI: 10.22044/jme.2026.17439.3463

کلمات کلیدی

بهینه‌سازی آتش‌باری
یکپارچه‌سازی معدن و کارخانه (معدن تا کارخانه)
شبکه‌های عصبی مصنوعی
پیش‌بینی خردایش (قطعه‌بندی سنگ)
تحلیل حساسیت

چکیده

طراحی انفجار مؤثر برای راندمان خردایش پایین‌دست بسیار مهم است. با این حال، مدل‌سازی تأثیر آن بر تولید مبتنی بر اندازه به دلیل تعاملات پیچیده و غیرخطی سنگ-خردشدگی همچنان چالش‌برانگیز است. این مطالعه با استفاده از شبکه‌های عصبی مصنوعی (ANN) بهینه‌شده، یک چارچوب یکپارچه از معدن تا آسیاب را برای پیش‌بینی تولید کل و خرد شده بر اساس اندازه (۰-۴۰ میلی‌متر، ۴۰-۸۰ میلی‌متر) از پارامترهای انفجار در مجتمع سنگ آهک سرآسیاب، ایران، توسعه داد. مجموعه داده‌ها شامل ۵۵ مشاهده صنعتی واقعی پس از پیش‌پردازش است. دو الگوریتم بهینه‌سازی، الگوریتم ژنتیک (GA) و بهینه‌سازی ازدحام ذرات (PSO)، برای افزایش عملکرد ANN به کار گرفته شدند. ANN بهینه‌سازی‌شده با PSO، تعمیم‌پذیری بسیار بهتری را نشان داد و به RMSE آزمایشی ۱۳۴۱.۸ (در مقابل ۱۵۴۹.۵ برای GA)، MAE 1108.9 (در مقابل ۱۲۶۰.۴) و R^2 0.9487 (در مقابل ۰.۸۹۳۷) دست یافت. تحلیل اهمیت ویژگی مبتنی بر حساسیت، پیش‌بینی‌کننده‌های غالب را کمّی کرد: مقدار ماده منفجره امولایت ۱۸.۴ ٪، تعداد تقویت‌کننده‌ها ۱۴.۹٪ و پارامترهای هندسی کلیدی (میانگین عمق، قطر و فاصله سوراخ) در مجموع بیش از ۴۱٪ را تشکیل دادند. در مقابل، متغیرهای سیستم شروع مانند طول قشر مغز، همبستگی خطی بالایی (r = -0.91) اما اهمیت پیش‌بینی حداقلی (۱.۵٪) نشان دادند. این نتایج تأکید می‌کنند که انرژی انفجاری و توزیع آن، نه فقط پیکربندی شروع انفجار، محرک‌های اصلی خروجی مبتنی بر اندازه هستند. این چارچوب داده‌محور، ابزاری عملی برای همسوسازی طراحی انفجار با نیازهای پردازش فراهم می‌کند و مستقیماً از کاهش انرژی و پایداری تولید در معدنکاری روباز پشتیبانی می‌کند.

نویسنده مسئول مکاتبات: v.shojaei@uk.ac.ir (و. شجاعی)